EPJ Web of Conferences **117**, 10007 (2016) DOI: 10.1051/epjconf/201611710007
NN2015

Detector developments for the Super-FRS

C. Nociforo[1], F. Schirru[1], M. Kiš[1] and S. Schlemme[1,2]

[1] GSI Helmholtzzentrum fr Schwerionenforschung, Darmstadt, Germany
[2] TU Darmstadt, Darmstadt, Germany

Abstract

Some developments of Super-FRS focal plane detector prototypes and results of recent in-beam tests performed at GSI and LNS-INFN with diamond detectors are presented.

1 Introduction

The magnetic in-flight separator Super-FRS [1] under construction at FAIR consists of 2-degrader stages, the pre-separator made mainly of normal conducting magnets and the main separator made of superconducting magnets. As shown in Fig. 1, it can deliver high energy radioactive beams (RIBs) starting from 20 Tm to the high-energy branch, slowed down RIBs to the low-energy branch (the beam can be even stopped at the end of the energy buncher) and pulsed RIBs for in-ring experiments. The right combination of beam energies and target/degrader thickness will typically let to optimize the delivery of in-flight highly-charged well separated fragments. Even though a strong reduction of contaminants is ensured at the end of the three branches, the particle rate in the first half of the main separator can still be high (1-10 MHz). Various combinations of the magnetic sections of the Super-FRS operated in dispersive, achromatic or dispersion-matched spectrometer modes will allow measurements of momentum distributions of secondary reaction products with high precision [2]. Due to the different experiments and operation modes a large variety of detectors is foreseen. All

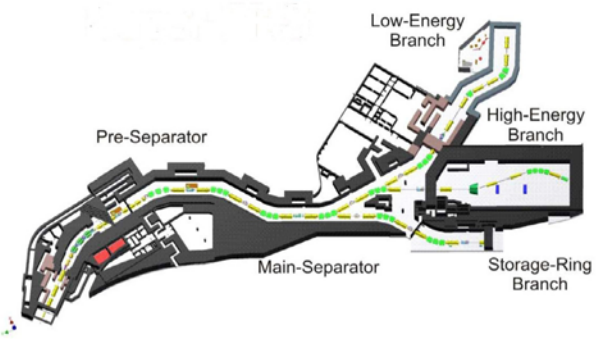

Figure 1: Layout of the Super-FRS.

this has strong implication on the design of the Super-FRS detecting system, which has to cope with two main technical challenges: high intensity and resolution.

2 Super-FRS radiation-hard detectors

2.1 Tracking detectors

The identification of different isotopes at the Super-FRS requires a combined event-by-event analysis of the magnetic rigidity (Bρ), time-of-flight (ToF) and energy deposition [3]. Toward the higher beam intensity we plan to use a set of Time Projection Chambers (TPC) with GEM (Gas Electron Multiplier) amplification. In addition to high resolution and adjustable gain over a wide range (from protons to Z=92), these detectors have the advantage of being able to perform particle tracking on an event-by-event basis exposing very little additional material to the ion beam. Considerable progress has been made in the past years in the development of GEM-TPC tracking detector prototypes [4] for the Super-FRS. Even though gas detectors are very robust against beam bombardment, they are too slow for timing measurements.

2.2 Time-of-flight detectors

The use of radiation hard silicon and diamond detectors for fast timing at Super-FRS has been recently exploited. A few experiments have been carried out in order to assess the ToF performances of radiation detectors

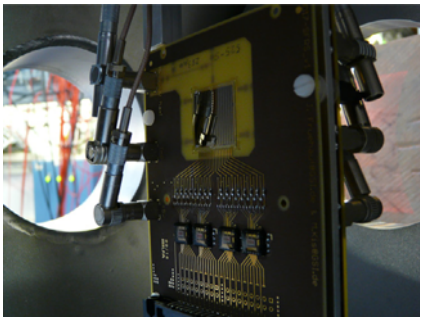

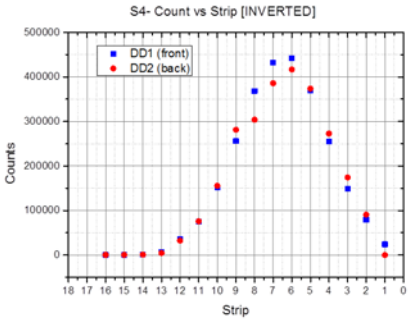

Figure 2: Left panel: PADI7 board with strip diamond detectors (front and back) Right panel: Horizontal beam profile reconstructed on diamonds.

based on diamond material. We have developed position-sensitive diamond detectors made of polycrystalline CVD (chemical vapour deposition) material of (20x20x0.3) mm^3 size provided by Element Six. Their electrodes were fabricated in house in 16-strips geometry by depositing on both sides of the diamond samples Cr/Au layers of thickness 50/100 nm respectively. The vertical geometry was chosen to match the horizontal dispersion of the separator. The device was mounted on a new board (see Fig. 2) having bias voltages, threshold and integrated amplification stage and able to provide LVDS output signals.

3 Beam tests measurements

3.1 ToF measurements

In August 2014, a test experiment was performed at the FRS [5] in GSI with ^{197}Au primary beam using a diamond pair as start and stop detectors, in experimental condition similar to those expected at the Super-FRS. A printed circuit board equipped with four PADI7 chips [6] and fabricated in house was used to readout each single diamond strip. The digital output signals from PADI after splitting were sent to the FPGA TDC VFTXs [7] synchronized with a 200 MHz external clock [1]. An example of beam profile reconstructed with two diamond detectors DD1 and DD2 located at the end of the FRS is shown in Fig. 2. A ToF resolution σ_{ToF} of about 40 ps has been measured between two strips of the front and back diamonds (see Fig. 3). A ToF resolution of about 50 ps was measured

[1]PADI and VFTX electronics had an intrinsic resolution below 15 ps.

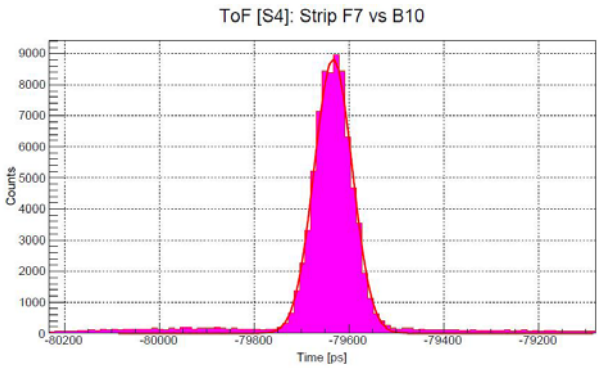

Figure 3: Diamond ToF measurement.

after positioning the DD2 detector at the mid-focal plane of the separator, about 35 m apart. The intrinsic time resolution of each diamond could be extracted taking advantage of the presence of the FRS TPC detectors [9] and plastics scintillator mounted along the beam line. After applying a TPC position correction, an intrinsic resolution $\sigma_t = \sigma_{ToF}/\sqrt{2} \approx 25$ ps is achieved.

3.2 Irradiation tests

Damage studies on the same diamond material have been also performed. At the LNS-INFN laboratory, a polycrystalline CVD diamond detector (pcCVD-DD) 0.3 mm thick has been irradiated via series of long irradiations of 10^7 $^{12}C/mm^2/s$ at 62 MeV/u. The detector has four squared metalized faces Q_{1-4} (10x10) mm^2 each. Each of them was connected to a broadband DBA amplifier [8]. The time resolution and the charge collection efficiency of the pcCVD-DD have been monitored via digital scope during low intensity runs taking place at the end of each series. Digital waveforms have been registered also for a single-crystal diamond detector (scCVD-DD) 0.09 mm thick, which was moved in during each low intensity run. The diamond analogue signals were split and sent to the channels of a oscilloscope (10 GS/s) and to a scaler after leading-edge discriminator for counting. All detectors worked inside a vacuum chamber at a pressure of 10^{-7} mbar. A collimator with 2.6 mm diameter was used at the entrance of the chamber. The beam current was measured by using an ionization chamber located behind the diamonds. The pcCVD-DD was kept constantly biased at 300 V since no change in the leakage current was observed. The number of ions counted by each squared section summed up during the long irradiation se-

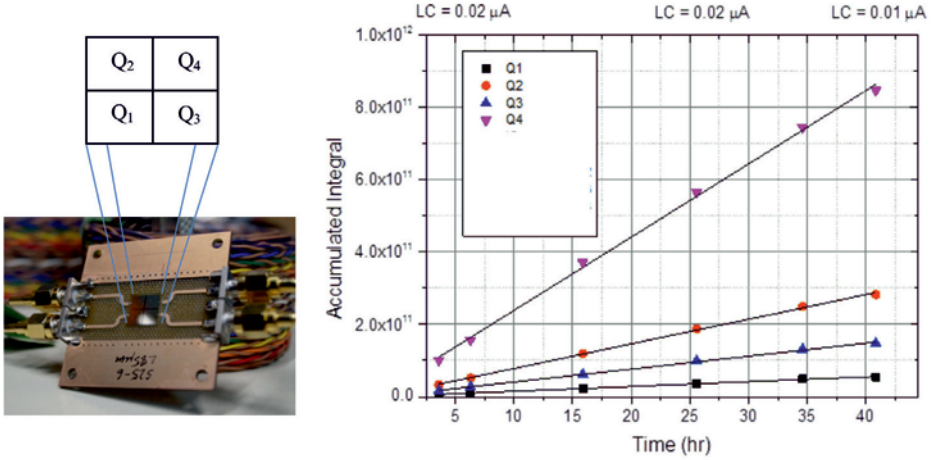

Figure 4: Left panel: pcCVD-DD with four squared faces Q_{1-4}. Right panel: Count numbers measured by each face of the pcCVD-DD during the irradiation measurement.

ries is shown in Fig. 4. Their sum provides a minimum accumulated dose of about 1.7 MGy corresponding to 4.3x10^9 ^{238}U/mm^2 s at 350 MeV/u (≈400 days operation of Super-FRS). Detector efficiency corrections will be taken into account to estimate the final accumulated dose. In Fig. 5 the slope (left side) and the amplitude (right side) distributions of Q_4 signals measured after 1 hour and 40 hours of irradiation are shown. Pulses below 30 mV have been discarded. The slope distribution was obtained by a linear fit of the sampled waveform at 10-90% of the maximum amplitude. From the present results, no degradation of the pcCVD-DD signal is observed within the 500 ps resolution (due to the DBA use). Preliminary results on the ToF measured between the scCVD-DD and Q_4 pcCVD-DD showing no change in the time resolution are also encouraging.

4 Future developments

The active area of the Super-FRS ToF detectors ranges from 10 up to 10^4 mm^2, depending on the focal planes. Not only material choice is important. Additional experimental requirements like multi-channel electronics and data acquisition need to be considered in relation to the increasing number of channel and amount of digitised data. In the next future not

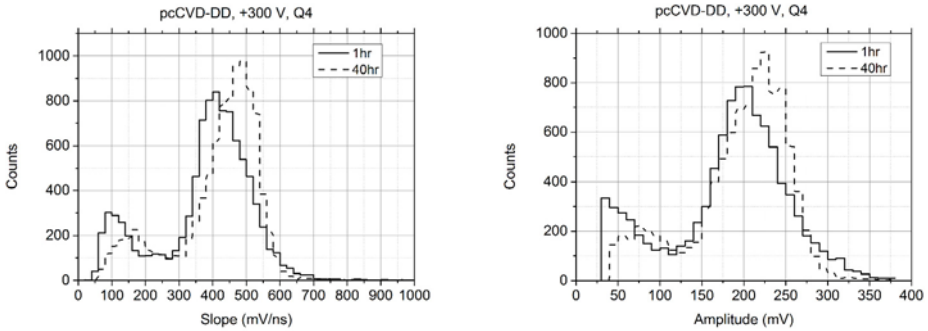

Figure 5: Pulse slope (left panel) and amplitude (right panel) of pcCVD diamond detector after 1 hour and 40 hours of irradiation.

only further irradiation tests with uranium ions will be performed but time measurements based via high precision time distribution and time stamps.

Acknowledgments

The authors wish to acknowledge the support of: M. Ciobanu, J. Frühauf and N. Kurz in providing the PADI and VFTX electronics, M. Träger and R. Visinka for detector processing, A. Kratz, P. Figuera, A. Musumarra and S. Salamone during the experiment at LNS-INFN.

References

[1] M. Winkler et al., Nucl. Instr. and Meth. B 266 (2008) 4183.

[2] J. Äystö et al., JPS Conf. Proc. 6, 020035 (2015).

[3] C. Nociforo, 2014 JINST 9 C01022.

[4] F. Garcia et al., GSI Report 2014, in press.

[5] H. Geissel et al., Nucl. Instr. and Meth. B 70 (1992) 286.

[6] M. Ciobanu et al., IEEE T-NS 61 (2014) 1015.

[7] E. Bayer and M. Traxler, IEEE T-NS 58 (2011) 1547.

[8] P. Moritz et al., Diamond and Related Materials 10 (2001) 1765.

[9] R. Janik et al., Nucl. Instr. and Meth. A 640 (2011) 54.